**Non-cell autonomous OTX2 transcription factor regulates anxiety-related behaviors in the mouse**

C. Vincent[1]*, J. Gilabert-Juan[1]*, D. Alvarez-Fischer[2,3], A.A. Di Nardo[1†], M.-O. Krebs[4,5,6], G. Le Pen[4] & A. Prochiantz[1†]

[1]Centre for Interdisciplinary Research in Biology (CIRB), Collège de France, CNRS UMR 7241, INSERM U1050, Labex MemoLife, PSL Research University, Paris, France.
[2]Institute of Neurogenetics, University of Lübeck, Lübeck, Germany
[3]Department of Psychiatry and Psychotherapy, University of Lübeck, Lübeck, Germany
[4]INSERM, Laboratoire de Physiopathologie des maladies Psychiatriques, UMR S1266 Institut de Psychiatrie et Neurosciences de Paris, Université Paris Descartes, Paris, France.
[5]Institut de Psychiatrie, CNRS GDR 3557, Paris, France.
[6]Faculté de Médecine Paris Descartes, Service Hospitalo Universitaire, Centre Hospitalier Sainte-Anne, Université Paris Descartes, Paris, France.

*C.V. and J.G.-J. contributed equally to this work.

†Corresponding authors: ariel.dinardo@college-de-france.fr, alain.prochiantz@college-de-france.fr

**SUMMARY**

The Otx2 homeoprotein transcription factor is expressed in the dopaminergic neurons of the ventral tegmental area, a mesencephalic nucleus involved in the control of complex behaviors through its projections to limbic structures, including the ventral hippocampus, amygdala, nucleus accumbens and prefrontal cortex. We find adult mice heterozygous for *Otx2* show a hypoanxious phenotype in light-dark box and elevated plus maze paradigms. However, the number of dopaminergic neurons, the integrity of their axons, their projection patterns in target structures, and the amounts of dopamine and dopamine metabolites in targets structures were not modified in the *Otx2* mutant. Because OTX2 is expressed by the choroid plexus, secreted into cerebrospinal fluid and transferred to parvalbumin interneurons of the cortex, hippocampus, and amygdala, we investigated if the hypoanxiety of *Otx2* heterozygous mice could result from the decreased synthesis of Otx2 in the choroid plexus. Indeed, hypoanxious phenotype was reversed by the overexpression of Otx2 specifically in choroid plexus of adult *Otx2* heterozygous mice, while hypoanxious phenotype could be induced in adult wild type mice by lowering OTX2 levels in the cerebrospinal fluid. Taken together, OTX2 synthesis by the choroid plexus followed by its secretion into the cerebrospinal fluid is an important regulator of the anxiety phenotype in the mouse.

## INTRODUCTION

Homeoprotein (HP) transcription factors are expressed during development when they participate in all developmental decisions, in and outside the nervous system (1). In the developing nervous system HPs are more specifically involved in the segmentation of the neuroepithelium, cell lineage decisions, cell shape and migration, and axon guidance (2). Interestingly, most HPs remain expressed in the adult nervous system in regions and cell types that differ from those identified during development and in relation with their specific and partially mysterious adult physiological functions (2; 3).

An aspect of HP functions that has recently attracted some attention is their ability to transfer between cells. This intercellular transport results in non-cell autonomous HP regulation of gene expression and potentially induces changes in the epigenetic status of the receiving cells (3). Although HP transduction *in vivo* and *in vitro* was only verified for about 15 HPs, the sequences responsible for HP internalization and secretion are highly conserved, strongly suggesting that transduction is a shared property of most of the 200-300 members of the HP family (4; 5).

The vertebrate *orthodenticle* orthologue *Otx2* homeogene encoding OTX2 HP acts, early in development, as a gap gene for the anterior part of the central nervous system, including the telencephalon (6; 7). However, *Otx2* expression is rapidly turned off and has already ceased in the mouse cerebral cortex parenchyma at embryonic day 15 (E15). In contrast, its expression persists throughout life in the pineal gland, choroid plexus (ChP), and in neurons within the septum, thalamus, cerebellum and midbrain, including the mesencephalic dopaminergic (mDA) neurons of the ventral tegmental area (VTA) (2). This latter observation indicates a possible implication in psychiatric disorders, as the VTA mDA neurons innervate several cerebral structures regulating complex behaviors (8; 9) and require *Otx2* expression for their proper development and survival (10; 11).

A role for Otx2 in the post-natal adult control of complex traits, such as depression or anxiety has recently been demonstrated by maternal separation experiments. For example, maternal separation of mouse pups between a critical period, ranging from postnatal day 10 (P10) to P20, leads to a social defeat-induced depressive adult phenotype regulated by a transient decrease in *Otx2* expression in the VTA (12). In a separate study also involving maternal separation-induced anxiety, it was proposed that *Otx2* upregulation in the ChP and OTX2 transfer to ventral hippocampus inhibitory interneurons may participate in the anxiety phenotype (13).

In the latter context, it must be recalled that OTX2 expressed in the ChP is secreted into the cerebrospinal fluid (CSF) and transported to the brain parenchyma where it is primarily captured by the fast-spiking GABAergic parvalbumin neurons (FSPV cells) (14). This capture is favored by the presence within OTX2 of a sequence (the RK-peptide) that recognizes specific extracellular glycosaminoglycans present in the perineural nets (PNNs) that enwrap FSPV cells in layers III and IV of the cerebral cortex (15; 16).

During mouse late postnatal development, the privileged accumulation of OTX2 within FSPV cells in the visual cortex opens plasticity for binocular vision at P20 and closes it by P40 (17). This critical period of plasticity is thus regulated by non-cell autonomous OTX2, a phenomenon that was recently extended to the auditory cortex and medial prefrontal cortex (mPFC) (18). For the visual cortex, it was also shown that pharmacological or genetic decreases of FSPV cell OTX2 content in the adult cortex reopens a window of plasticity, allowing for the recovery of binocular vision in mice made amblyopic by the closure of one eye during the juvenile critical period (14; 15).

The accumulation of ChP-derived OTX2 in layers III/IV FSPV cells throughout the adult cortex suggests that this transfer may regulate complex behaviors. This hypothesis is supported by recent studies in the *Otx2-AA* mouse line in which the arginine-lysine (RK) doublet of the RK-peptide necessary for addressing OTX2 specifically to FSPV cells was mutated into two alanines (AA doublet). This RK->AA mutation slows down OTX2 accumulation in FSPV cells throughout the cerebral cortex. This delays the maturation of the primary auditory cortex and the mPFC, resulting in prolonged acquisition of acoustic preference in adulthood linked to anxiolysis (18).

In the present study, we have taken advantage of the *Otx2* heterozygote mouse line (*Otx2-het*) in which one *Otx2* allele is replaced by GFP leading to a decrease in *Otx2* expression (19). We find that lowered *Otx2* expression modifies anxiety-related behaviors and that anxiety is regulated by secretion of OTX2 at the level of the ChP.

## MATERIAL AND METHODS

### Ethics statement

All animal procedures, including housing, were carried out in accordance with the recommendations of the European Economic Community (86/609/EEC), the French National Committee (87/848) and French bylaws (AGRG1240332A / AGRG1238724A / AGRG1238767A / AGRG1238729A / AGRG1238753A). For surgical procedures, animals were anesthetized with Xylazine (Rompun 2%, 5 mg/kg) and Ketamine (Imalgene 500, 80 mg/kg). This research (project no. 00704.02) was approved by Ethics committee n° 59 of the French Ministry for Research and Higher Education.

### Mice

The *Otx2-het* mouse line was generated in the laboratory of Antonio Simeone (CEINGE, Naples), with the *Otx2* coding sequence and introns replaced by *GFP* (20). $Otx2^{+/GFP}$ males were crossed with B6D2F1 females to obtain *Otx2-het* mice. The single-chain antibody (scFv) OTX2 knock-in *scFv-Otx2* mouse line was generated by the Institut Clinique de la Souris (Strasbourg, France) by inserting the *scFv-Otx2* minigene construct in the *Rosa26* locus (21). Mice were raised in a 12-hour light/dark cycle with 2 to 5 (males) or 6 (females) animals per cages. Temperature was controlled (21±3°C), and food and water provided ad libitum.

### AAV injections

Adeno-associated viruses (AAV) were generated by Vector Biolabs: AAV5(CMV)-HAOtx2-2A-mCherry and AAV5(CMV)-mCherry. Stereotaxic injections were performed with a Hamilton syringe at a rate of 0.3 µl/min: 2 µl/lateral ventricle (bregma: x = ±1.28 mm, y = -0.58 mm, z = 2 mm). Mice were tested in the light-dark box and on the elevated-plus maze 3 and 4 weeks after injection, respectively.

### Cre-TAT protein injection

Stereotaxic injection (bregma: x = -0.58 mm, y = ±1.28 mm, z = 2 mm) of Cre-TAT in 15% DMSO into the lateral ventricles of anesthetized mice was performed with a Hamilton syringe at a rate of 0.2 µl/min as previously described (14). Mice were tested in the elevated-plus maze 4 weeks after injection.

### Behavior

Tests were performed from P90 to P120 in groups of female or male WT and *Otx2-het* mice in the following order: locomotor activity, Y-maze, elevated-plus maze, light-dark box, rotarod,

tail-suspension, prepulse inhibition, forced swimming test. Except for rotarod, tail-suspension and prepulse inhibition tests, behavior was registered using a semi-automated infrared system (Viewpoint, Lyon).

*Y maze*
Short-term spatial memory and locomotor activity was evaluated by the spontaneous alternative exploration of the Y-maze during 10 min. The maze consisted of 3 alleys diverging at 120° from one another, 40 cm long, 15 cm width, with black 30 cm high Perspex borders decorated differently in each arm, which were illuminated at 50 lux. The mouse was placed at the tip of one arm and the time spent visiting each of the other arms sequentially was counted as a memory performance.

*Elevated-plus maze*
A cross-shape maze elevated at 70 cm from the floor was illuminated at 50 lux. Two "closed" arms facing each other and protected by black Perspex walls (20 cm high), are crossed perpendicularly by the two "opened" unprotected arms. The mouse was placed at the center of the cross and activity was recorded for 10 min. The time spent in the open arms taken as an index of low anxiety.

*Light-dark box*
Boxes are composed of a dark (black walls, floor and roof) and light (white walls and floor, no roof, 150 lux) compartments of equal volume (20 x 20 x 30 cm) linked by a small opening. The mouse is placed in the light box facing the opening, and anxiety is measured by the time spent in the dark compartment over a 10 min test.

*Rotarod*
Equilibrium and motor coordination were measured in a progressively accelerating (from 2 to 40 rpm during 5 min) rotarod (model 47600, Ugo Basile, Italy). Each daily test included 3 trials separated by 90 min intervals, during 2 days.

*Tail-suspension test*
Mice were suspended by the tail with adhesive linked to a gauge detecting movement (automated system BIOSEB, France), during 6 min. Immobility was interpreted a sign of depression.

*Forced swimming test*
This test evaluates depressive behaviors by registering the periods of freezing of mice placed in a see-through Perspex cylinder full of water (25°C). The cylinder is 25 cm high, 13 cm in diameter and filled up to 20 cm. On the first day, the mice were habituated to the test during 10 min, on the second day the test lasted 6 min. An infrared panel positioned vertically behind the cylinder detects mice movements. Immobility was interpreted a sign of depression.

*Prepulse Inhibition test*
Testing was carried out in a SR-Lab system (San Diego Instruments, USA). Each mouse was placed in a startle chamber. Acoustic noise bursts were presented via a speaker mounted 26 cm above the tube. Throughout the session, a background noise level of 68 dB was maintained. After a 5-min acclimatization period (68 dB background noise), 10 startle pulses (120 dB, 40 ms duration) were presented with an average inter-trial interval of 15 s. During the next 20 min, no stimulus (background noise, 68 dB), prepulses alone (72, 76, 80 or 84 dB, 20 ms duration), startle pulses alone, and prepulses followed 80 ms later by startle pulses were presented 10

times, randomly distributed. Percent prepulse inhibition (PPI) was calculated as [100 – 100x(startle response of acoustic startle from acoustic prepulse and startle stimulus trials)/(startle response alone trials)].

**Dosage of cerebral amines and their metabolites**

Brains were dissected in ice-cold PBS and dry tissue was kept at -80°C. Extracts were prepared and analyzed by HPLC using a reverse phase column (Nucleosil 120-3 C18; Knauer) with electrochemical detection as described (22). Data were recorded and quantified using HPLC Chromeleon computer system (Dionex).

**Immunohistochemistry**

Anesthetized mice were perfused transcardially with 20 ml of PBS and 30 ml of 4% paraformaldehyde (10 ml/min). Dissected brains were post-fixed in 4% paraformaldehyde at 4°C for 1 h, rinsed in PBS, soaked in 20% sucrose at 4°C for 12-24 h and frozen. Fluorescent immunohistochemistry was performed on cryostat sections (20 µm). Briefly, after permeabilization with 1% Triton for 20 min, sections were incubated in 100 mM Glycine for 20 min, blocked with PBS, 0.2% Triton, 10% normal goat serum (NGS) for 45 min and incubated overnight with primary antibodies: anti-tyrosine hydroxylase antibody (rabbit, abcam, 1/500); anti-dopamine transporter (rat, Millipore, 1/5000); anti-c-Fos (rabbit, Cell Signaling, 1/200); anti-parvalbumin (rabbit, Swant, 1/500); anti-tryptophan hydroxylase 2 (rabbit, abcam, 1/500) in PBS, 1% Triton, 3% NGS at 4°C. After 3 washes in PBS, 1% Triton, secondary antibodies were used (Alexa Fluor-conjugated, Molecular Probes) for 2 h at room temperature (1/2000). After 3 washes in PBS, 1% Triton, sections were mounted in Dapi-fluoromount medium and kept at 4°C. DAB Immunohistochemistry was performed on free-floating cryostat sections (40 µm). Endogenous peroxidase was removed with a 5 min incubation in 0.3% $H_2O_2$, 0.2% Methanol. Sections were permeabilized and blocked as above and incubated during 12-24h with an anti-tyrosine hydroxylase antibody (rabbit, Pel Freeze Biologicals, 1/1000) in PBS, 0.1% Triton, 3% NGS at 4°C. After 3 washes in PBS, 0.1% Triton, a biotin-coupled anti-rabbit antibody (1/2000) was added for 2h at room temperature. After 3 washes in PBS, 0.1% Triton, biotin was detected by using the Vectastain Elite ABC HRP kit and Peroxidase Substrate kit (1h of ABC buffer + reaction with DAB) from Vectorbiolabs and the slides washed in $ddH_2O$.

**Cell counting and fibers density**

Images from the immunohistochemistry sections were acquired with a Leica SP5 confocal microscope at 10X or 40X and analyzed with FIJI/ImageJ. For the VTA cell counting, every second section (containing VTA) was counted by stereology using Stereo Investigator software (MBF Bioscience Inc.) at a 40X magnification. Amygdala was imaged between Bregma -1.7 mm and -2.60 mm. Confocal z-stacks covering the whole depth of the sections were taken with 3 µm step size and only subsets of confocal planes with the optimal penetration level for each antibody were selected. After z-projection of stacks, the basolateral amygdala area was selected and measured and the number of cells was determined in the area for each marker and the density of the staining was assessed by the mean grey value option of FIJI.

**Statistical Analysis**

All statistics were performed using GraphPad Prism (version 8.1.2, GraphPad Software). In order to avoid type II errors, outliers were defined as more than 2 standard deviations from the group mean and were removed from analysis. Main effects and interactions with more than 2 groups were determined using analyses of variance (ANOVA) or 2-way ANOVA with Tukey's multiple comparison *post hoc* test. Student's *t* test was used for single comparisons among two groups. An alpha level of 0.05 was used for all statistical tests.

## RESULTS

### *Otx2*-heterozygote mice present low anxiety-related behaviors

Three-month-old *Otx2-het* (one allele of *Otx2*) and their wild-type siblings were analyzed for motor coordination (rotarod), depression (tail-suspension and forced swimming tests), cognition (Y-maze), sensorimotor gating (prepulse inhibition) and anxiety (openfield, light-dark box and elevated-plus maze). Motor coordination measured by the rotarod test showed differences between males and females ($F(3.270)=28.50$ $p<0.0001$), but not between WT and *Otx2-het* animals (Figure 1A). Depression measured by the forced swimming (Figure 1B) and tail suspension (Figure 1C) tests showed no differences between the two genotypes and a small difference between males and females in the tail suspension test only (77.09 ± 12.84 vs 39.09 ± 5.41; $F(1.52)=10.40$ $p=0.0022$), with females being more depressed than males. The short-term spatial memory test (Y maze) was used to measure both locomotor activity and memory. Although females show a slightly higher motor activity (4944 ± 130 vs 4439 ± 160; $F(1.54)=4.75$ $p=0.0337$), here again no differences were found between the two phenotypes (Figure 1D). Another absence of difference between genotypes was found in the prepulse inhibition (PPI) test (Figure 1E), although the startle amplitude was a bit higher in mutant males at 120 decibels only (38.60 ± 5.19 vs 71.87 ± 13.27 $p<0.0001$). All in all, it can be concluded that the loss of one *Otx2* allele does not affect motor activities, cognition, depression behavior or sensorimotor gating.

In contrast, strong differences between WT and *Otx2-het* mice appeared in the light-dark box (LDB) and the elevated plus maze (EPM) anxiety tests (Figure 2A, B). *Otx2-het* mice spent more time than WT in the lit compartment of the LDB (58.84 ± 9.64 vs 115.93 ± 13.87; $F(1.57)=11.34$ $p=0.0014$) as well as in the open arms of the EPM (6.00 ± 1.44 vs 46.13 ± 8.71; $F(1.52)=18.49$ $p<0.0001$). These effects are similar in both sexes as revealed by the absence of significant sex x genotype effect in each test (Figure 2B). The EPM test was also conducted in absence of light (Figure 2C) ensuring that the hypo-anxious behavior associated with the loss of one *Otx2* allele is independent of a putative vision deficit created by decreased *Otx2* expression (6.86 ± 1.78 vs 25.34 ± 5.67; $F(1.42)=10.09$ $p=0.0028$). The EPM anxiety test was thereafter used as an anxiety read-out in all experiments.

### The low anxiety behavior of *Otx2-het* mice in the EPM test does not reflect a dopaminergic or serotoninergic phenotype

In a previous study, it was found that mice heterozygous for *Engrailed-1*, a homeogene expressed in the mDA neurons of the ventral midbrain, experience a progressive loss of these neurons in the Substantia Nigra (SNpc) and VTA beginning at 6 weeks. This results in a 40% and 20% neuronal loss at 48 weeks in the SNpc and VTA, respectively (23). Otx2 is expressed in the adult VTA (11), and the projections of the VTA into several target structures, including the hippocampus, nucleus accumbens, amygdala, and the mPFC may be involved in anxiety regulation (12). This led us to analyze the hypoanxiety behavior of *Otx2-het* mice between 1 and 4 months of age, including the age at which behavior was tested (3 months). Figure 2D illustrates that the hypoanxiety behavior is established very early and is maintained during this period, making it unlikely that it is due to mDA progressive neuronal loss ($F(3.229)=56.06$ $p<0.0001$; 1 mo $p=0.03$; 2 mo $p=0.0019$; 3 mo $p=0.032$; 4 mo $p<0.0001$).

The latter conclusion was further confirmed by stereology counting of tyrosine hydroxylase (TH)-positive cell bodies of the VTA (Figure 3A) which showed no differences between 3-month-old *Otx2*-het animals and their WT siblings. However as illustrated in a study on SNpc mDA neurons in WT and *Engrailed-1* heterozygotes, cells bodies can be present while axons

begin degenerating as characterized by their fragmentation, clearly visible both in the medial forebrain bundle and in the striatum (24). Hence, we evaluated the state and density of the TH- and dopamine transporter (DAT)-positive fibers in the basolateral amygdala, a region responsible for the fear response and receiving mDA terminals from the VTA (25). No significant changes were observed neither for the density of any of the two markers of dopaminergic neurotransmission, nor for the morphology of the fibers (Figure 3C, D).

To further evaluate a possible dopaminergic phenotype, dopamine (DA) and its main metabolites dihydroxyphenylacetic acid (DOPAC) and homovanillic acid (HVA) were measured in the cortex (anterior and posterior), the striatum, and the hippocampus of 3-month-old WT and *Otx2*-het mice from the same litter (Figure 3B). The amounts are very similar in both genotypes and in all studied structures, thus eliminating both a change in absolute DA concentrations and in DA metabolism.

Early Otx2 hypo-morphism can also lead to an increase in the number serotonin (5HT) neurons by an anterior shift in the midbrain/hindbrain boundary (26; 27). Because 5HT has is implicated in anxiety regulation (28; 29), we measured the levels of 5HT and of its main metabolite 5HIAA. We found no differences between animals of either genotype and in any of the studied structures (Figure 3E). Furthermore, the serotoninergic fibers in the amygdala marked with the TPH2 antibody showed similar morphology and density in both WT and *Otx2*-het mice (Figure 3C, D).

**Otx2 synthesized in the ChP and released into the CSF regulates mouse anxiety**

In postnatal mice, *Otx2* is expressed in several extra-cortical structures, including the VTA and ChP (12; 14) but no expression takes place in the cerebral cortex parenchyma (17). Although not expressed in the cerebral cortex, OTX2 is imported from extra-cortical structures, in particular ChP, by neurons throughout the cortex (primarily PV cells), including limbic structures (14; 18). In addition to all studied cortical regions, including the mPFC, non-cell autonomous OTX2 can be identified in hippocampus CA1, and basolateral amygdala (14). Because of this presence of OTX2 in several structures implicated in the regulation of anxiety-related behaviors, we developed gain- and loss-of-function experiments to evaluate the possible contributions of the ChP to the regulation of anxiety behavior.

Adeno-associated virus-5 (AAV5) injected into the lateral ventricles (Figure 4A) gains specifically access to ChP (14) allowing a 1.5 fold overexpression of *Otx2* in this structure ($t$=3.525; p=0.0023) (Figure 4B). This overexpression resulted in a tendency of increased anxiety in the hypo-anxious phenotype of *Otx2-het* mice in the EPM test (Figure 4C, p=0.067). Despite the lack of significance, this experiment suggests that Otx2 expression in the ChP is sufficient to restore a normal anxiety behavior in the *Otx2-het* mouse.

ChP do not only clean the CSF from toxic metabolites acting as the 'kidney of the brain', but also nurture the brain by secreting into the CSF a large number of trophic factors (30; 31), including Otx2 (14). The restoring effect of expressing Otx2 in the ChP could thus result from the cell autonomous transcription of genes encoding factors secreted into the CSF and/or from the direct secretion of OTX2 into the CSF, similarly to what has been demonstrated in critical periods paradigms (14; 18; 21). To reinforce the ChP gain of function experiment (Figure 4C) and verify if OTX2 secreted by the ChP could regulate anxiety behavior, we took advantage of a mouse line expressing a secreted scFv directed against OTX2 (21). In this mouse, injection of a cell-permeable Cre recombinase in the brain ventricles induces the secretion of the scFv-OTX2 antibody at the level of the ChP (21). This leads to the neutralization of extracellular OTX2 in the CSF and, in the case of the visual cortex, to the reopening of plasticity (21). As

illustrated in Figure 4D, neutralizing ChP-derived OTX2 in the CSF installs a hypo-anxious phenotype in 3-month-old mice ($t$=2.120; p=0.039).

**DISCUSSION**

In this study, we provide evidence for a role of Otx2 in the regulation of anxious behavior and that OTX2 secreted from the ChP into the CSF plays a role in this regulation. This does not exclude other extra-cortical sources, in particular the pineal gland, but establishes that the ChP, through the synthesis and secretion of OTX2 is an important anxiety regulator. Anxiety regulation can be the consequence of modest changes in OTX2 expression and/or secretion. For expression, the AAV5 strategy induces a 50% increase in ChP *Otx2* transcription. For secretion, previous studies using the same neutralization strategy in the CSF showed that a 20% OTX2 decrease in the visual cortex FSPV cells is sufficient to reopen plasticity in the adult (21). In the present study, target structures were not identified, but it can be claimed that an acute decrease of OTX2 en route from the ChP to the brain parenchyma of 3-month-old mice is enough to decrease anxiety. This result excludes that *Otx2-het* mice hypoanxiety is purely developmental, as also suggested by the similar hypo-anxious behavior of mice at 1, 2, 3 and 4 months of age.

As just mentioned, non-cell autonomous OTX2 target cells and structures were not investigated. In such complex behaviors, it is likely that several interacting structures are implicated. If so, the presence of OTX2 in the CSF could give the protein access to many candidate target structures functioning in association through the existence of neuronal networks and hub structures (32; 33). This is apparently the case as non-cell autonomous OTX2 was found in PV cells from the mPFC, hippocampus and amygdala (13; 14). Interestingly, recent experiments strongly suggest that OTX2 imported in PNN-enwrapped FSPV cells in the mPFC and in the ventral hippocampus might regulate anxiety (13; 18). Although the accent here is placed on PV cells, other interneurons might play an Otx2-associated role as suggested in the mPFC where OTX2 is mainly imported by PV+ and calretinin+ interneurons (70% and 20% co-labeling, respectively) (18).

The large repertoire of anxiety-related interconnected target structures is also shared by projections from the VTA(8; 9). Since Otx2 is expressed in the adult VTA and may regulate the survival of the mDA cells that constitute 65% of the neuronal population in this structure (34), a possible cell autonomous role of OTX2 on VTA mDA neuron physiology/survival or, alternatively, a non-cell autonomous effect on their hippocampal of cortical targets following anterograde transport and trans-synaptic passage cannot not be excluded. The experiments demonstrating that the number of mDA neurons is not affected in the mutant at 3 months of age (the hypo-anxious phenotype is present already at 1 months and persists at least for 3 more months) is not in favor of the idea that mDA neuron number is at the origin of the phenotype. In addition, we found no change in the amount of DA and DA metabolites in the cortex, hippocampus and striatum, further supporting the view that the mDA "phenotype" is not altered in *Otx2-het* mice. Nor did we find any change in 5HT innervation or the amount of 5HT and of its metabolite 5HIAA as expected if the early *Otx2* hypomorphism had shifted the midbrain/hindbrain boundary in a more anterior position (26; 27).

However, the results from Nestler and colleagues (12), establishes a role for cell autonomous Otx2 in the VTA, independently of the number of mDA neurons or of DA levels and metabolism. They showed that a transient decrease in Otx2 expression between P10 and P20 in mDA neurons of the VTA can trigger a depressive state in adulthood following social defeat. Our finding that overexpression Otx2 in the ChP can reduce anxiety in the adult suggests that

the mechanisms involved in the present hypo-anxiety phenotype either differs from those at work in the maternal separation paradigm or that a link exists between *Otx2* expression in the VTA during a critical period (here from P10 to P20) and the ability of the ChP to direct OTX2 to non-cell autonomous target structures. Results from the Gould and colleagues further support this possibility (13). They observed a parallel increase of OTX2 in the ChP and in ventral hippocampus PV cells of mice made hyperanxious through early maternal separation.

Together, the findings from the Nestler, Gould and our labs encourages us to propose a model outlined in Figure 5. We hypothesize that Otx2 expression, at the mRNA and protein level, in VTA mDA neurons constitutes a first trigger for an enhanced transfer into target PV cells (ventral hippocampus, mPFC, or other region) of OTX2 from extra-cortical sources, including ChP. Conversely an abnormal decrease in *Otx2* expression during a critical period would jeopardize the proper development of mood-associated circuits. This is very reminiscent of how eye opening at P14 in the mouse is followed by a transient critical period in the binocular visual cortex, the opening and duration of which is regulated by extra-cortical OTX2. The trigger that comes from the eye at P14 is dependent on OTX2 in the retina (17), suggesting that OTX2 locally regulates the expression of factors acting on subcortical and cortical structures or, and non-exclusively, is itself transported to visual cortex PV cells (35; 36). The latter view is supported by the finding that recombinant OTX2 injected in the eye can reach PV cells in the visual cortex (35). Whatever the signals might be, we speculate that they provoke the first assembly of PNNs allowing for further import of OTX2 from extra-cortical sources (15). In brief, the VTA would play the role in the early regulation of complex behaviors that the eyes play in the regulation of plasticity in the primary visual cortex. Given the huge body of literature on sensory system plasticity, this hypothesis, if confirmed by future experiments, would foster new views on the study of "mood" regulation and disease.

**Acknowledgments and Disclosures**
We would like to thank Chantal Dubreuil and Jessica Apulei for technical assistance. Funding was provided by Fondation Bettencourt Schueller, European Research Council Advanced Grant (HOMEOSIGN, ERC-2013-ADG-339379 to A.P.), and Agence Nationale de la Recherche Grant (ANR-11-BLAN-069467 to A.P.). A.A.D. and A.P. are consultants for BrainEver. All other authors report no biomedical financial interests or potential conflicts of interest.

## REFERENCES

1. Bürglin TR, Affolter M (2016): Homeodomain proteins: an update. *Chromosoma*. 125: 497–521.
2. Prochiantz A, Di Nardo AA (2015): Homeoprotein Signaling in the Developing and Adult Nervous System. *Neuron*. 85: 911–925.
3. Di Nardo AA, Fuchs J, Joshi RL, Moya KL, Prochiantz A (2018): The Physiology of Homeoprotein Transduction. *Physiol Rev*. 98: 1943–1982.
4. Joliot A, Prochiantz A (2004): Transduction peptides: from technology to physiology. 6: 189–196.
5. Prochiantz A, Joliot A (2003): Can transcription factors function as cell-cell signalling molecules? *Nat Rev Mol Cell Biol*. 4: 814–819.
6. Acampora D, Mazan S, Lallemand Y, Avantaggiato V, Maury M, Simeone A, Brûlet P (1995): Forebrain and midbrain regions are deleted in Otx2-/- mutants due to a defective anterior neuroectoderm specification during gastrulation. *Development*. 121: 3279–3290.
7. Simeone A, Acampora D, Mallamaci A, Stornaiuolo A, D'Apice MR, Nigro V, Boncinelli E (1993): A vertebrate gene related to orthodenticle contains a homeodomain of the

bicoid class and demarcates anterior neuroectoderm in the gastrulating mouse embryo. *EMBO J*. 12: 2735–2747.
8. Beier KT, Steinberg EE, DeLoach KE, Xie S, Miyamichi K, Schwarz L, *et al.* (2015): Circuit Architecture of VTA Dopamine Neurons Revealed by Systematic Input-Output Mapping. *Cell*. 162: 622–634.
9. Morales M, Margolis EB (2017): Ventral tegmental area: cellular heterogeneity, connectivity and behaviour. *Nat Rev Neurosci*. 18: 73–85.
10. Chung CY, Licznerski P, Alavian KN, Simeone A, Lin Z, Martin E, *et al.* (2010): The transcription factor orthodenticle homeobox 2 influences axonal projections and vulnerability of midbrain dopaminergic neurons. *Brain*. 133: 2022–2031.
11. Di Salvio M, Di Giovannantonio LG, Acampora D, Prosperi R, Omodei D, Prakash N, *et al.* (2010): Otx2 controls neuron subtype identity in ventral tegmental area and antagonizes vulnerability to MPTP. *Nat Neurosci*. 13: 1481–1488.
12. Peña CJ, Kronman HG, Walker DM, Cates HM, Bagot RC, Purushothaman I, *et al.* (2017): Early life stress confers lifelong stress susceptibility in mice via ventral tegmental area OTX2. *Science*. 356: 1185–1188.
13. Murthy S, Kane GA, Katchur NJ, Lara Mejia PS, Obiofuma G, Buschman TJ, *et al.* (2019): Perineuronal Nets, Inhibitory Interneurons, and Anxiety-Related Ventral Hippocampal Neuronal Oscillations Are Altered by Early Life Adversity. *Biol Psychiatry*. doi: 10.1016/j.biopsych.2019.02.021.
14. Spatazza J, Lee HHC, Di Nardo AA, Tibaldi L, Joliot A, Hensch TK, Prochiantz A (2013): Choroid-plexus-derived Otx2 homeoprotein constrains adult cortical plasticity. *Cell Rep*. 3: 1815–1823.
15. Beurdeley M, Spatazza J, Lee HHC, Sugiyama S, Bernard C, Di Nardo AA, *et al.* (2012): Otx2 binding to perineuronal nets persistently regulates plasticity in the mature visual cortex. *Journal of Neuroscience*. 32: 9429–9437.
16. Miyata S, Komatsu Y, Yoshimura Y, Taya C, Kitagawa H (2012): Persistent cortical plasticity by upregulation of chondroitin 6-sulfation. *Nat Neurosci*. 15: 414–422.
17. Sugiyama S, Di Nardo AA, Aizawa S, Matsuo I, Volovitch M, Prochiantz A, Hensch TK (2008): Experience-dependent transfer of Otx2 homeoprotein into the visual cortex activates postnatal plasticity. *Cell*. 134: 508–520.
18. Lee HHC, Bernard C, Ye Z, Acampora D, Simeone A, Prochiantz A, *et al.* (2017): Genetic Otx2 mis-localization delays critical period plasticity across brain regions. *Mol Psychiatry*. 22: 680–688.
19. Bernard C, Kim H-T, Torero Ibad R, Lee EJ, Simonutti M, Picaud S, *et al.* (2014): Graded Otx2 activities demonstrate dose-sensitive eye and retina phenotypes. *Hum Mol Genet*. 23: 1742–1753.
20. Acampora D, Di Giovannantonio LG, Di Salvio M, Mancuso P, Simeone A (2009): Selective inactivation of Otx2 mRNA isoforms reveals isoform-specific requirement for visceral endoderm anteriorization and head morphogenesis and highlights cell diversity in the visceral endoderm. *Mech Dev*. 126: 882–897.
21. Bernard C, Vincent C, Testa D, Bertini E, Ribot J, Di Nardo AA, *et al.* (2016): A Mouse Model for Conditional Secretion of Specific Single-Chain Antibodies Provides Genetic Evidence for Regulation of Cortical Plasticity by a Non-cell Autonomous Homeoprotein Transcription Factor. (J. M. Hébert, editor) *PLoS Genet*. 12: e1006035.
22. Alvarez-Fischer D, Henze C, Strenzke C, Westrich J, Ferger B, Höglinger GU, *et al.* (2008): Characterization of the striatal 6-OHDA model of Parkinson's disease in wild type and alpha-synuclein-deleted mice. *Exp Neurol*. 210: 182–193.

23. Sonnier L, Le Pen G, Hartmann A, Bizot J-C, Trovero F, Krebs M-O, Prochiantz A (2007): Progressive loss of dopaminergic neurons in the ventral midbrain of adult mice heterozygote for Engrailed1. *Journal of Neuroscience*. 27: 1063–1071.
24. Nordströma U, Beauvais G, Ghosh A, Pulikkaparambil Sasidharan BC, Lundblad M, Fuchs J, *et al.* (2015): Progressive nigrostriatal terminal dysfunction and degeneration in the engrailed1 heterozygous mouse model of Parkinson's disease. *Neurobiol Dis*. 73: 70–82.
25. Beier KT, Gao XJ, Xie S, DeLoach KE, Malenka RC, Luo L (2019): Topological Organization of Ventral Tegmental Area Connectivity Revealed by Viral-Genetic Dissection of Input-Output Relations. *Cell Rep*. 26: 159–167.e6.
26. Brodski C, Weisenhorn DMV, Signore M, Sillaber I, Oesterheld M, Broccoli V, *et al.* (2003): Location and size of dopaminergic and serotonergic cell populations are controlled by the position of the midbrain-hindbrain organizer. *Journal of Neuroscience*. 23: 4199–4207.
27. Millet S, Campbell K, Epstein DJ, Losos K, Harris E, Joyner AL (1999): A role for Gbx2 in repression of Otx2 and positioning the mid/hindbrain organizer. *Nature*. 401: 161–164.
28. Santangelo AM, Sawiak SJ, Fryer T, Hong Y, Shiba Y, Clarke HF, *et al.* (2019): Insula serotonin 2A receptor binding and gene expression contribute to serotonin transporter polymorphism anxious phenotype in primates. *Proc Natl Acad Sci USA*. 116: 14761–14768.
29. Adhikari A, Topiwala MA, Gordon JA (2010): Synchronized activity between the ventral hippocampus and the medial prefrontal cortex during anxiety. *Neuron*. 65: 257–269.
30. Lun MP, Monuki ES, Lehtinen MK (2015): Development and functions of the choroid plexus-cerebrospinal fluid system. *Nat Rev Neurosci*. 16: 445–457.
31. Nedergaard M (2013): Neuroscience. Garbage truck of the brain. *Science*. 340: 1529–1530.
32. Tovote P, Fadok JP, Lüthi A (2015): Neuronal circuits for fear and anxiety. *Nat Rev Neurosci*. 16: 317–331.
33. Lüthi A, Lüscher C (2014): Pathological circuit function underlying addiction and anxiety disorders. *Nat Neurosci*. 17: 1635–1643.
34. Di Salvio M, Di Giovannantonio LG, Omodei D, Acampora D, Simeone A (2010): Otx2 expression is restricted to dopaminergic neurons of the ventral tegmental area in the adult brain. *Int J Dev Biol*. 54: 939–945.
35. Sugiyama S, Prochiantz A, Hensch TK (2009): From brain formation to plasticity: insights on Otx2 homeoprotein. *Dev Growth Differ*. 51: 369–377.
36. Rebsam A, Mason CA (2008): Otx2's incredible journey. *Cell*. 134: 386–387.
37. Kaufman J, Wymbs NF, Montalvo-Ortiz JL, Orr C, Albaugh MD, Althoff R, *et al.* (2018): Methylation in OTX2 and related genes, maltreatment, and depression in children. *Neuropsychopharmacology*. 43: 2204–2211.

## FIGURE LEGENDS

**Figure 1. Behavioral phenotype characterization of the *Otx2-het* mice**.
Male and female WT or *Otx2*-het mice were subjected to numerous behavior tests between P90 and P120. (A) The rotarod test measured the latency to fall (sec) from a progressively accelerating rotating rod from 2 to 40 rpm during 5 min trial (WT females n=16; WT males n=18; *Otx2-het* females n=10; *Otx2-het* males n=14). (B) Forced swim test measured total time immobile (sec) during a 6 min period in a small pool (WT females n=16; WT males n=17; *Otx2-het* females n=10; *Otx2-het* males n=14). (C) Tail suspension test measured total time immobile (sec) during a 6 min period (WT females n=16; WT males n=17; *Otx2-het* females n=10; *Otx2-het* males n=15). (D) Total locomotor activity (min) and amount of time spent in alternative arms (in %) were measured in the Y-maze during 10 min (WT females n=16; WT males n=17; *Otx2-het* females n=10; *Otx2-het* males n=15). (E) Prepulse inhibition (PPI) test performed in a startle chamber to measure startle response amplitude (lower panels) and PPI (%, upper panels) (WT females n=16; WT males n=18; *Otx2-het* females n=10; *Otx2-het* males n=14). Data are presented as mean ± SEM.: *p < 0.05; **p < 0.01; ***p < 0.001; ****p < 0.0001 (two-way ANOVA, post hoc: Tukey´s test).

**Figure 2. Anxiety phenotype characterization of the *Otx2-het* mice.**
(A) The light-dark box test measured time (sec) spent in light box during a 10 min period (WT females n=15; WT males n=16; *Otx2-het* females n=16; *Otx2-het* males n=14). (B) Total time (sec) spent in open arms in the elevated plus maze during a 10 min period (WT females n=15; WT males n=15; *Otx2-het* females n=15; *Otx2-het* males n=14). (C) Elevated plus maze performed in normal (50 lux) or dark (0 lux) conditions (WT light n=13; WT dark n=12; *Otx2-het* light n=11; *Otx2-het* dark n=12). (D) Elevated plus maze at different ages (from 1 month to 4 months) (WT 1 mo n=44; WT 2 mo n=39; WT 3 mo n=16; WT 4 mo n=33; *Otx2-het* 1 mo n=32; *Otx2-het* 2 mo n=35; *Otx2-het* 3 mo n=22; *Otx2-het* 4 mo n=31). Data are presented as mean ± SEM.: *p < 0.05; **p < 0.01; ***p < 0.001; ****p < 0.0001 (two-way ANOVA, post hoc: Tukey´s test).

**Figure 3. Dopaminergic and serotoninergic markers are not disturbed in the *Otx2-het* mice.**
(A) Immunohistochemistry for tyrosine hydroxylase (TH) in the *Otx2-het* (n=4) and WT (n=5) mice for quantification of VTA dopaminergic cells. Scale bar: 50 µm. (B) Quantification of metabolites related to the dopaminergic system (DA, Dopamine; DOPAC, 3,4-Dihydroxyphenylacetic acid; HVA, Homovanillic acid) in the anterior (Cx ant) and posterior cortices (Cx post), striatum (Str) and hippocampus (Hipp) (WT n=5; *Otx2-het* n=7). (C) Staining of fibers with dopamine (DAT, dopamine transporter; TH, tyrosine hydroxylase) and serotonin (TPH2, Tryptophan hydroxylase 2) in the basolateral amygdala in the *Otx2-het* and WT mice. Scale bar: 250 µm. (D) Quantification of DAT, TH and TPH2 fibers in the basolateral amygdala (WT n=6; *Otx2-het* n=7). (E) Quantification of metabolites related to the serotoninergic system (5HT, serotonin transporter; 5HIAA, 5-hydroxyindoleacetic acid) in the anterior (Cx ant) and posterior cortices (Cx post), striatum (Str) and hippocampus (Hipp) (WT n=5; *Otx2-het* n=7). Data are presented as mean ± SEM (student´s t test).

**Figure 4. Otx2 overexpression in ChP rescues the hypoanxious phenotype in the *Otx2-het* mice.**
(A) Schematic representation of the injection of AAV5(CMV)-HAOtx2-2A-mCherry virus in the ChP. In the image, the infected cells of the ChP expressing the fluorescent mCherry marker (white) compared to the control animals. Scale bar: 100 µm. (B) qRT-PCR of (mRNA) *Otx2*

(normalized by GAPDH) in the ChP tissue after 3-weeks viral expression (AAV-ctrl n=9; AAV-HAOtx2 n=12). (C) Time spent in open arms (sec) during a 10 min trial in the elevated plus maze for the control mice (WT; n=12), the *Otx2-het* mice injected in the ChP with control virus (AAV-ctrl; n=13) and the *Otx2-het* mice injected in the ChP with virus overexpressing Otx2 (AAV-HAOtx2; n=11). (D) Time spent in open arms (sec) during a 10 min trial in the elevated plus maze for the mutants expressing the single-chain antibody against OTX2 (scFv-Cre-Tat; n=23) and the controls not expressing the antibody (scFv-NaCl; n=34). Data are presented as mean ± SEM: #p = 0.067; *p < 0.05; **p < 0.01 (student´s t test or ANOVA).

**Figure 5. Hypothetical scheme for a VTA, limbic structures and ChP interaction**
The model proposes that *Otx2* in the VTA is upregulated in response to synaptic inputs or systemic signals (e.g. hormonal signals). Although this is not represented in this simplified illustration, the VTA is highly heterogeneous with compartments projecting to different structures (e.g anterior cingulate cortex, ventral hippocampus, amygdala, nucleus accumbens…) (25) and all compartments probably do not respond to similar signals in Otx2 regulation. The general principle is that, responding to the latter signals [Panel 1], Otx2 is upregulated and, either directly (35) or through the regulation of targets informs the corresponding limbic structures [Panel 2], more precisely the PV cells which, in response, assemble PNNs [Panel 3]. The latter assembly allows for OTX2 from extra-cortical sources (here the ChP) to recognize its binding sites within the PNNs (15), to enter the PV cells [Panel 4] and provoke their maturation. In the adult the permanent entry of OTX2 is necessary to maintain a differentiated state (2). Indeed, adult gain of OTX2 expression or neutralization of extracellular OTX2 at the level of the ChP modifies the anxiety phenotype of the mice (this study). In this hypothetical scheme based on studies on visual cortex critical period and adult plasticity (2), a specific traumatism modifying Otx2 expression in a VTA sub-compartment (for example maternal separation between a P10 and P20 critical period in the mouse) (12) may leave a permanent epigenetic trace on the functioning of physiologic circuits (37).

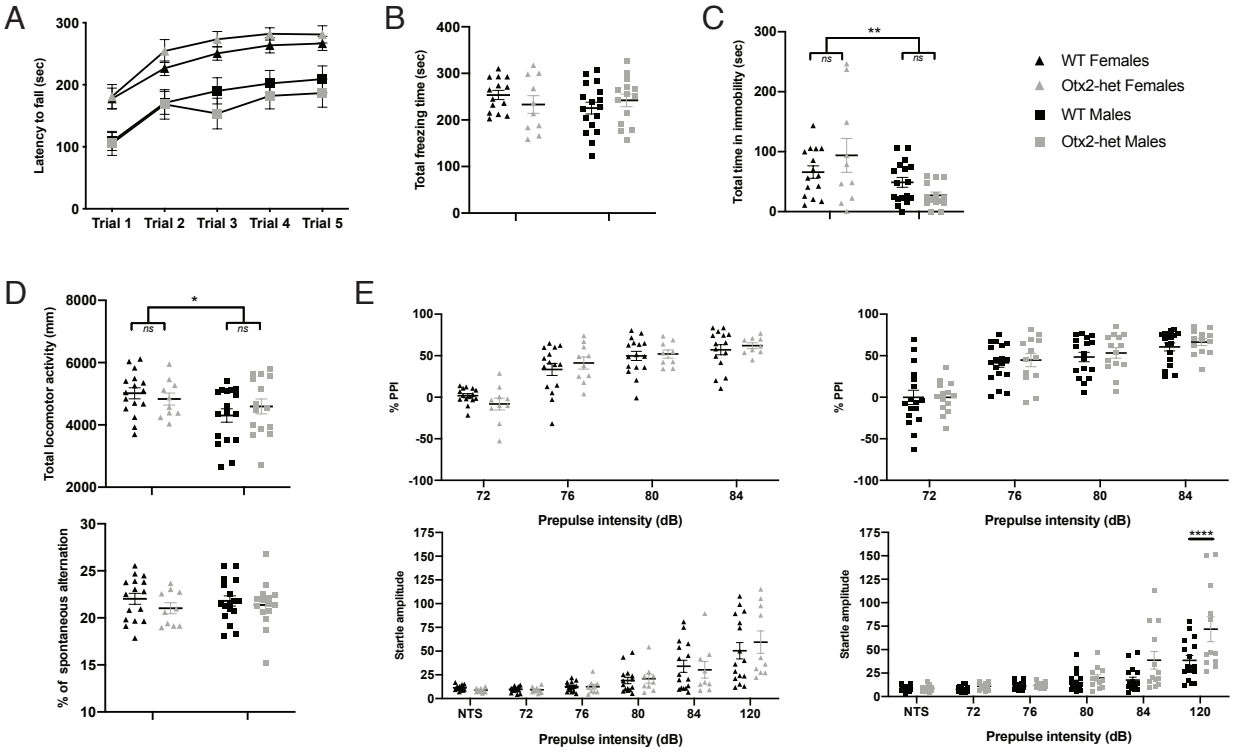
A
Latency to fall (sec)
Trial 1
Trial 2
Trial 3
Trial 4
Trial 5
B
Total freezing time (sec)
C
Total time in immobility (sec)
ns
ns
**
WT Females
Otx2-het Females
WT Males
Otx2-het Males
D
Total locomotor activity (mm)
ns
ns
*
% of spontaneous alternation
E
% PPI
Prepulse intensity (dB)
Startle amplitude
NTS
72
76
80
84
120
****

Figure 1

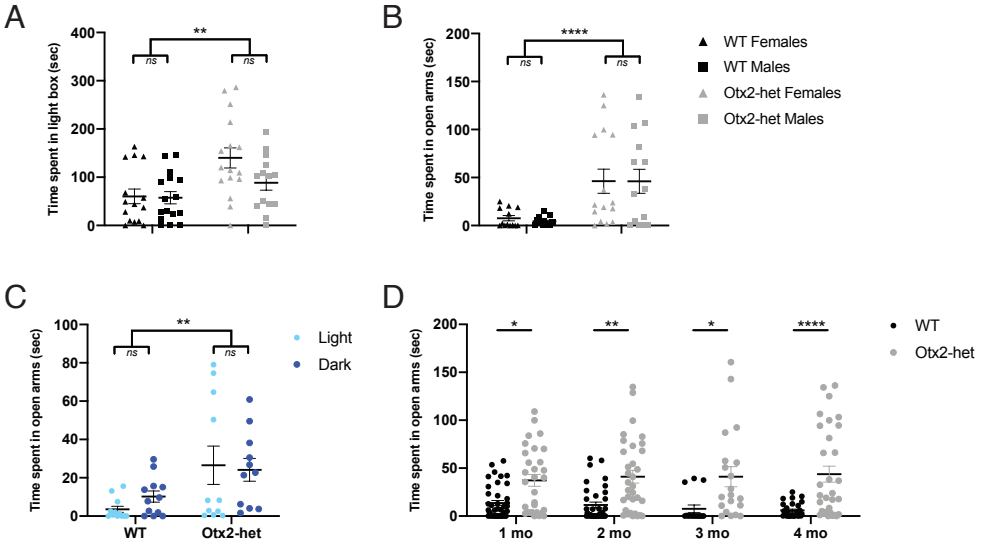
A
Time spent in light box (sec)
400
300
200
100
0
**
ns
ns
B
Time spent in open arms (sec)
200
150
100
50
0
****
ns
ns
WT Females
WT Males
Otx2-het Females
Otx2-het Males
C
Time spent in open arms (sec)
100
80
60
40
20
0
**
ns
ns
WT
Otx2-het
Light
Dark
D
Time spent in open arms (sec)
200
150
100
50
0
*
**
*
****
1 mo
2 mo
3 mo
4 mo
WT
Otx2-het

Figure 2

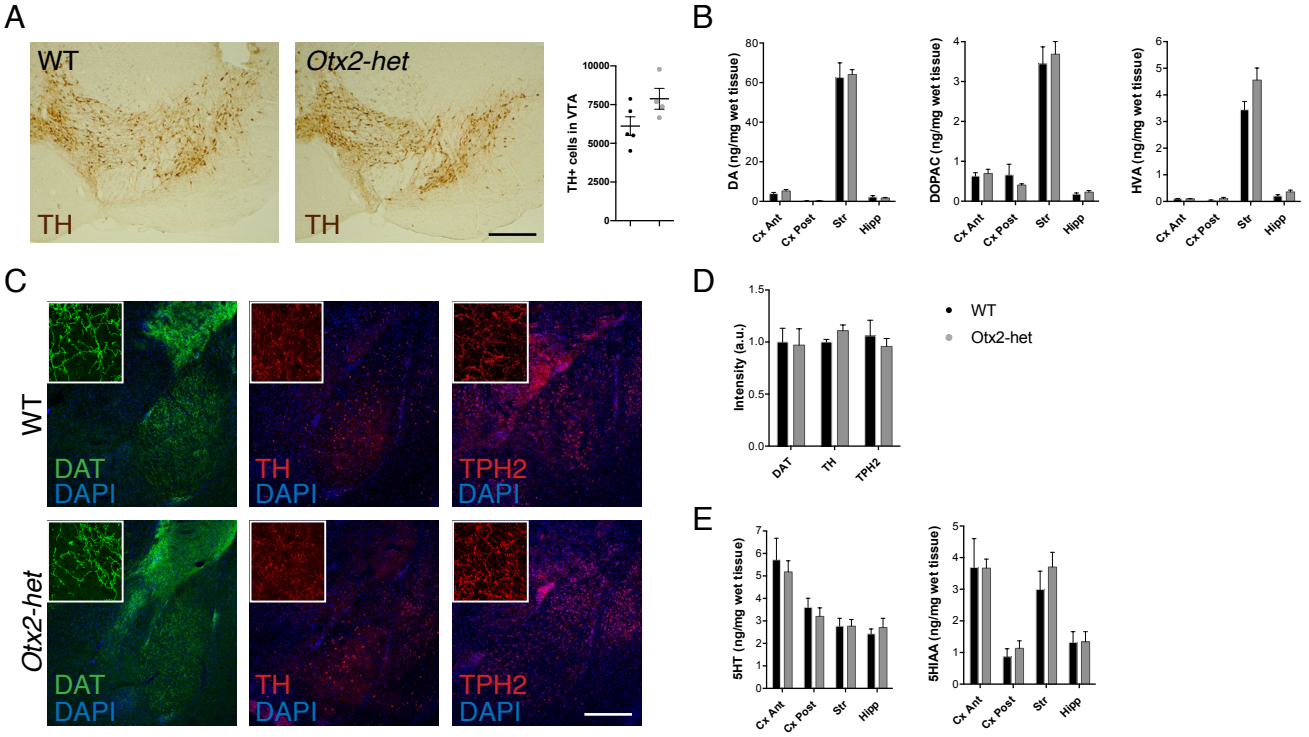
A
WT
Otx2-het
TH
TH
TH+ cells in VTA
B
DA (ng/mg wet tissue)
DOPAC (ng/mg wet tissue)
HVA (ng/mg wet tissue)
Cx Ant
Cx Post
Str
Hipp
C
WT
Otx2-het
DAT
DAPI
TH
DAPI
TPH2
DAPI
D
Intensity (a.u.)
DAT
TH
TPH2
WT
Otx2-het
E
5HT (ng/mg wet tissue)
5HIAA (ng/mg wet tissue)

Figure 3

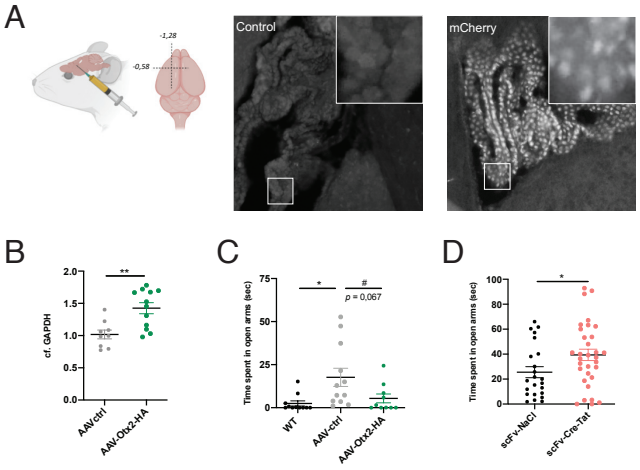
A
-1,28
-0,58
Control
mCherry
B
cf. GAPDH
2.0
1.5
1.0
0.5
0.0
**
AAV-ctrl
AAV-Otx2-HA
C
Time spent in open arms (sec)
75
50
25
0
*
#
p = 0,067
WT
AAV-ctrl
AAV-Otx2-HA
D
Time spent in open arms (sec)
100
80
60
40
20
0
*
scFv-NaCl
scFv-Cre-Tat

Figure 4

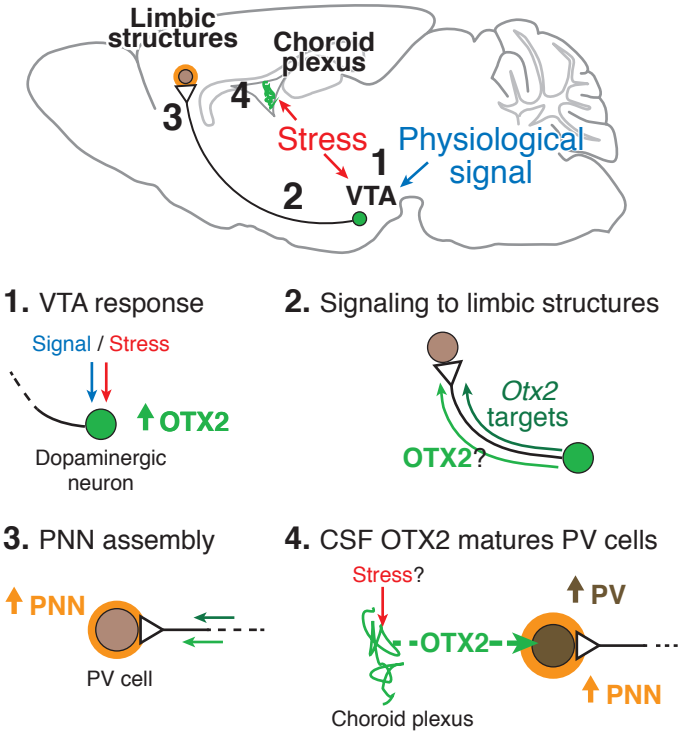
Limbic structures
Choroid plexus
3
4
Stress
1
Physiological signal
2
VTA
1. VTA response
Signal / Stress
OTX2
Dopaminergic neuron
2. Signaling to limbic structures
Otx2 targets
OTX2?
3. PNN assembly
PNN
PV cell
4. CSF OTX2 matures PV cells
Stress?
OTX2
PV
PNN
Choroid plexus

Figure 5